Supporting Information

Diaminomalenonitrile Functionalized Gelators in F^-/CN^- Sensing, Phase-Selective Gelation, Oil Spill Recovery and Dye Removal from Water

Rameez Raza, Atanu Panja and Kumaresh Ghosh*

Department of Chemistry, University of Kalyani, Kalyani-741235, India.
Email: ghosh_k2003@yahoo.co.in; kumareshchem18@klyuniv.ac.in.

Table S1. Results of gelation test for compounds **1** and **2**.

Solvent	**1**	**2**[1]
CH_3OH	I	I
DMF	S	S
$CHCl_3$	S	S
THF	S	S
DMSO	**G** (17 mg/mL, 58°C)	PS
CH_3CN	**G** (12 mg/mL, 56°C)	PS
Toluene	**G** (10 mg/mL, 74°C)	PG
Benzene	**G** (12 mg/mL, 66°C)	PG
1,2-dichlorobenzene	**G** (25 mg/mL, 48°C)	**G** (42 mg/mL, 44 °C)
DMSO-H_2O(1:1,v/v)	**G** (8 mg/mL, 66°C)	I
DMF-H_2O (1:1,v/v)	**G** (7 mg/mL, 64 °C)	**G** (10 mg/mL, 58 °C)
CH_3CN-H_2O (1:1,v/v)	PG	I
Pet ether*	**G** (15 mg/mL, 58°C)	**G** (26 mg/mL, 66°C)
Hexane*	**G** (14 mg/mL, 64°C)	**G** (27 mg/mL, 68°C)
Cyclohexane*	**G** (23 mg/mL, 62°C)	**G** (32 mg/mL, 70°C)
Petrol*	**G** (14 mg/mL, 58°C)	**G** (24 mg/mL, 72°C)
Kerosene*	**G** (16 mg/mL, 70°C)	**G** (25 mg/mL, 74°C)
Diesel*	**G** (14 mg/mL, 56°C)	**G** (24 mg/mL, 72°C)
Pump oil*	**G** (15 mg/mL, 72°C)	**G** (26 mg/mL, 76°C)
Silicon oil*	**G** (13 mg/mL, 68°C)	**G** (28 mg/mL, 72°C)

S = Solution; G = Gel (mgc, T_{gel}); I = Insoluble; PS = Partially soluble; P = Precipitation, PG = partial gel (thick material that did not stick on the top of the vial upon inversion). Gelation studies were carried out by taking upto 25 mg and 50 mg of compounds **1** and **2**, respectively in 1 ml of different solvents. Gels were primarily characterized by inversion of vial method after ~15 min of sample preparation.

* In these solvents compounds **1** and **2** were either insoluble or partially soluble. Gelation was investigated by adding THF solution of compounds **1** and **2** to these solvents at 1:19 ratio (THF: solvent, v/v) at concentration upto 30 mg/mL. Gels were primarily characterized by inversion of vial method after ~15 min of sample preparation.

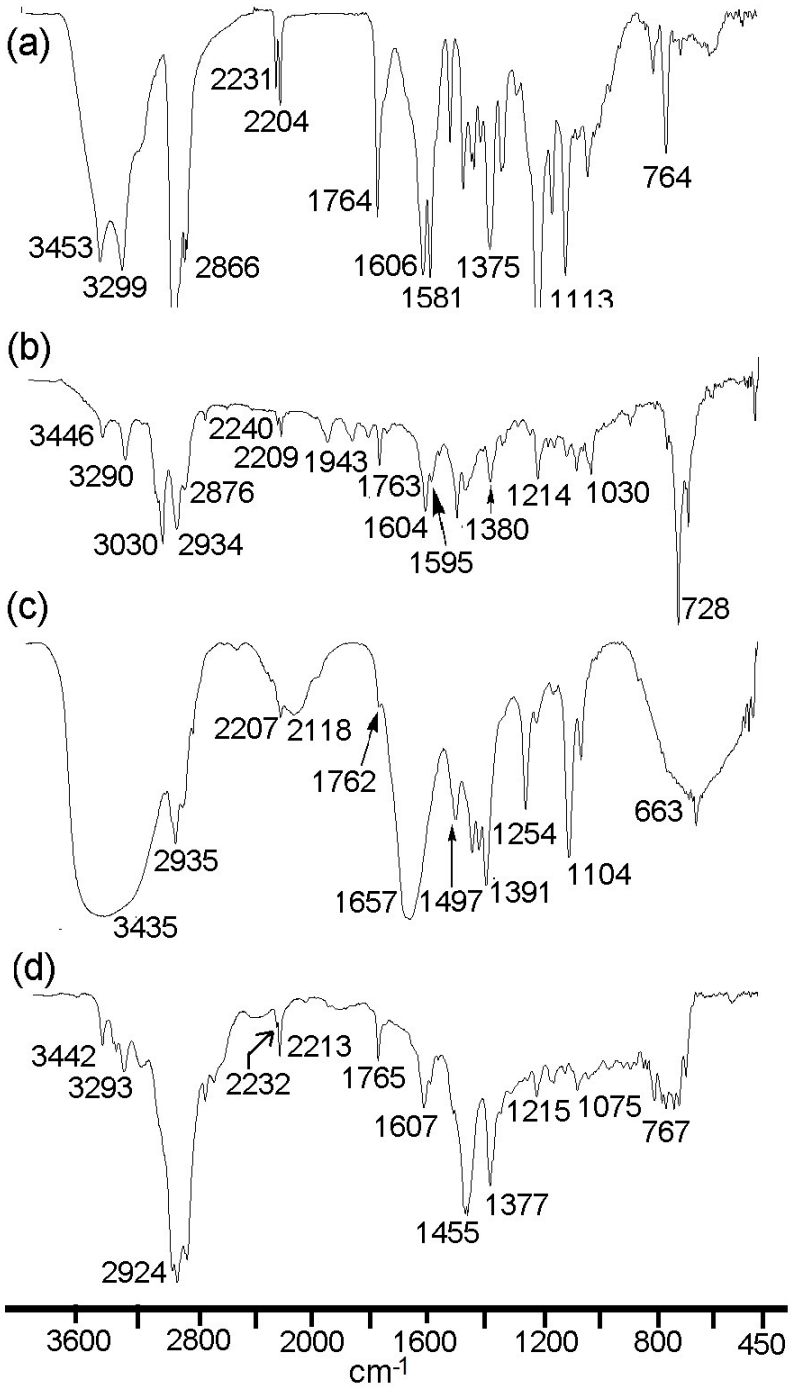

Fig. S1. Partial FTIR spectra of **1** in (a) amorphous state and gel states in (b) toluene, (c) DMF-H_2O (1:1, v/v) and (d) Kerosene.

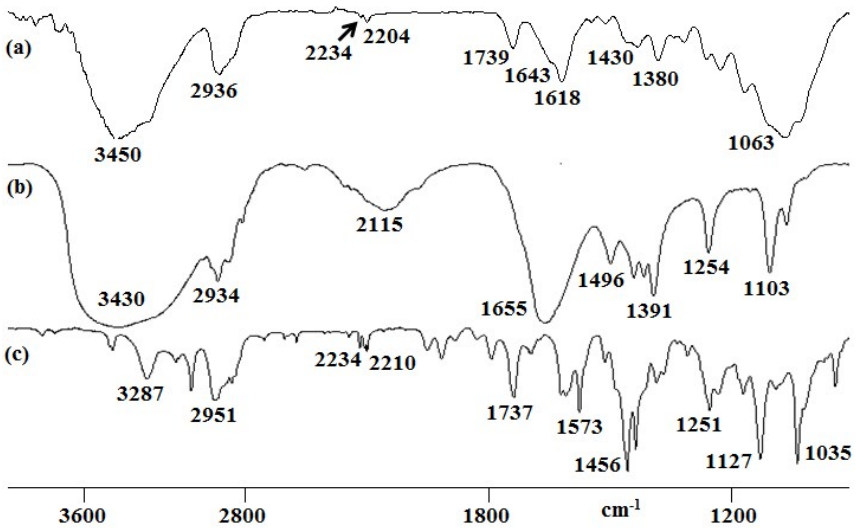

Fig. S2. Partial FTIR spectra of **2** in (a) amorphous state and gel states in (b) DMF-H_2O (1:1, v/v) and (c) 1,2-dichlorobenzene.[1]

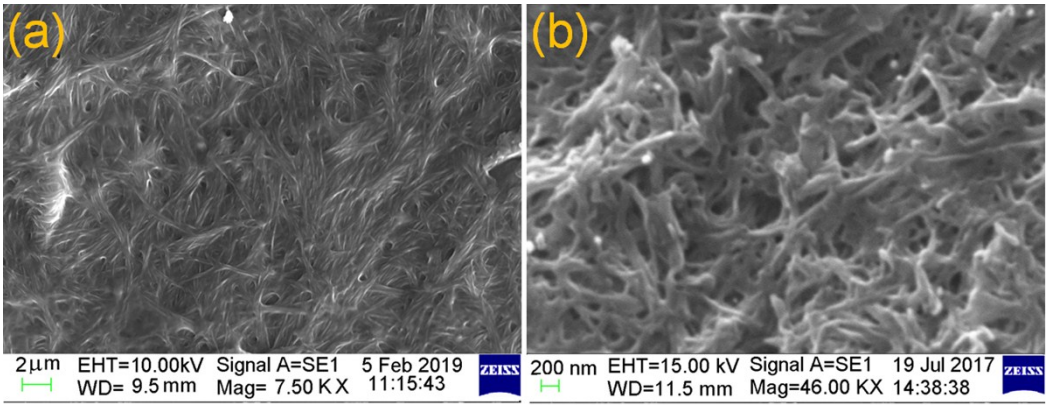

Fig. S3. SEM images of xerogel of (a) compound **1** and (b) compound **2** in DMF-H_2O (1:1, v/v)

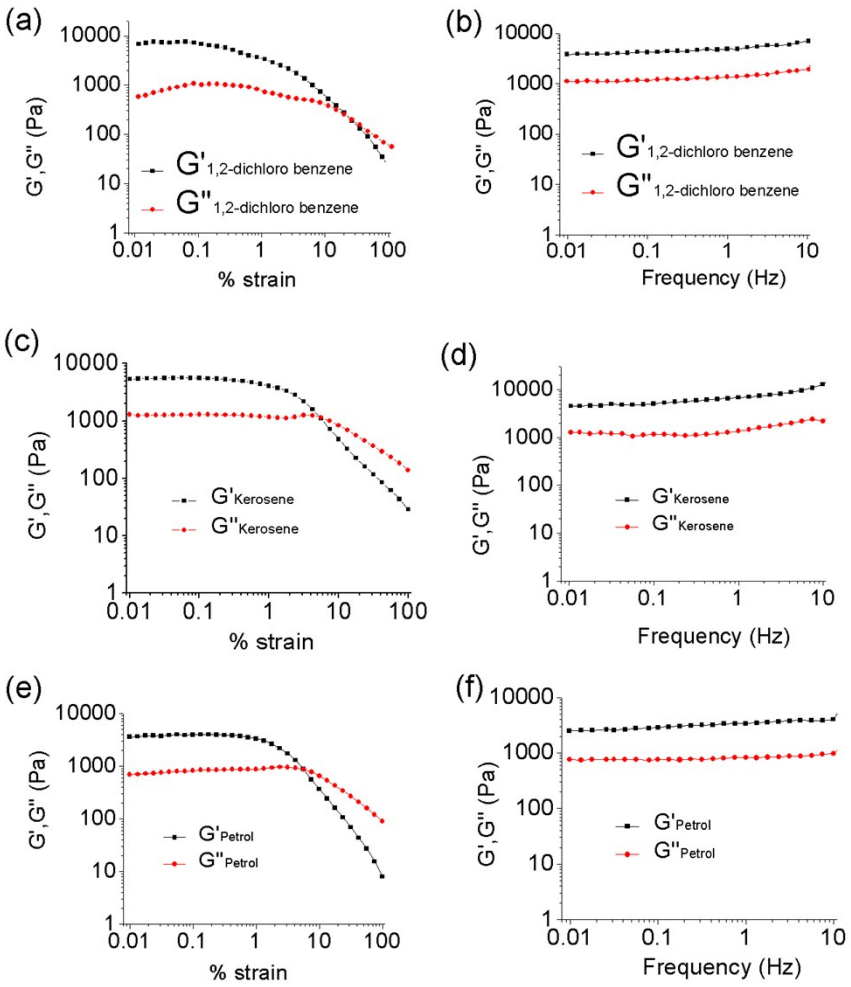

Fig. S4. Rheological studies of the gels of **1**; (a, c and e) amplitude sweep and (b, d and f) frequency sweep experiments. All the gels were prepared at respective mgc and the experiments were carried out at 25 ^{o}C. For all the gels, amplitude sweep experiment was carried out at constant frequency of 1Hz and frequency sweep experiment (except for the 1,2-dichlorobenzene gel) was performed at constant 0.1% strain. For the 1,2-dichlorobenzene gel, the frequency sweep experiment was carried out at constant 0.05% strain.

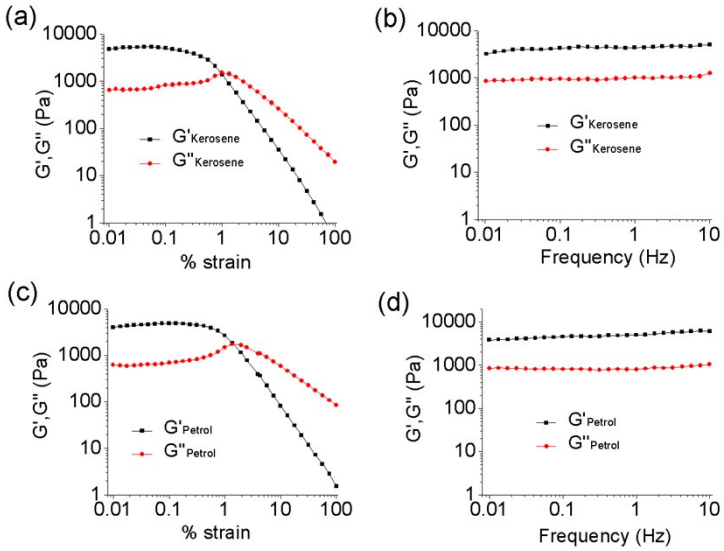

Solvent	Critical strain (%)	Crossover (% strain)	G'_{av} (Pa)*	G''_{av} (Pa)*	G'_{av}/G''_{av}
Kerosene	0.2	1.0	4325	968	4.46
Petrol	0.7	1.5	4883	849	5.75

* G'_{av} and G''_{av} values were calculated from frequency sweep data

Fig. S5. Rheological studies of the gels of **2**; (a and c) amplitude sweep and (b and d) frequency sweep experiments. All the gels were prepared at respective mgc and the experiments were carried out at 25 °C. For all the gels, amplitude sweep experiment was carried out at constant frequency of 1Hz and frequency sweep experiment was performed at constant 0.1% strain.

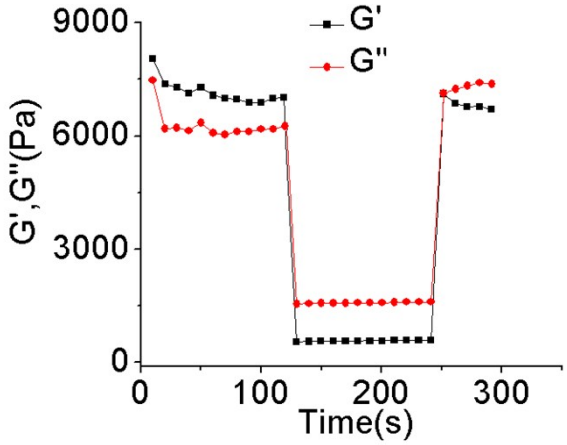

Fig. S6. Thixotropy-loop test via continuous step-strain measurements with the 1,2-dichlorobenzene gel of **2**. The gel was subjected to a sudden increase in strain from 0.05% (where G'>G") to 30% (where G'<G"). However, when the strain was reversed from high to low strain after a recovery period of 2 min still G" was higher than G' indicating dominance of sol-type nature. The experiment was carried out at 25 °C and the gel was pepared at 1.5 wt %, (w/v).

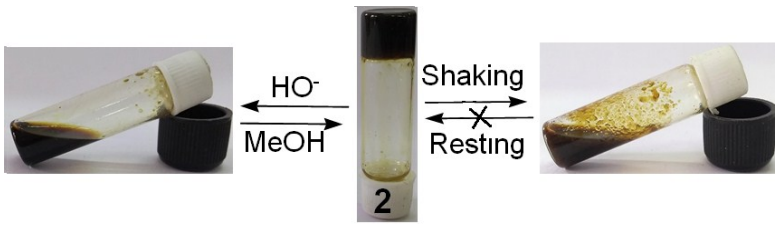

Fig. S7. Photograph showing the sol-gel interconversion of the 1,2-dichlorobenzene gel of **2** in the presence of different physical and chemical stimulus.

Fig. S8. Gel-to-sol transformation of **1** in Toluene upon addition of CN^- and F^- ions.

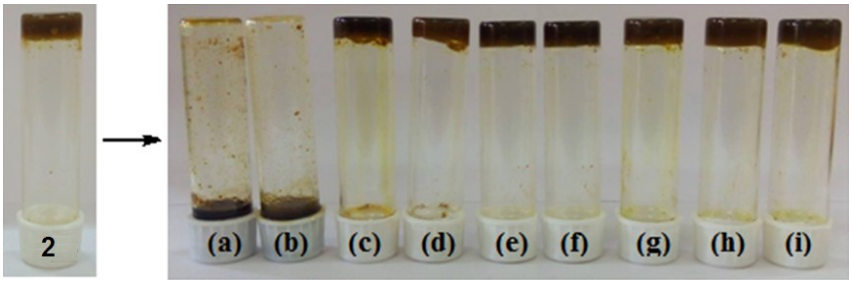

Fig. S9. Photograph showing the phase changes of **2** (at mgc) in 1,2-dichlorobenzene when the gels were prepared with equiv. amount of different anions (as tetrabutylammonium salts) [from left to right: (a) CN^-, (b)F^-, (c) AcO^-, (d) $H_2PO_4^-$, (e) Cl^-, (f) Br^-, (g) I^-, (h) NO_3^- and (i) HSO_4^-].

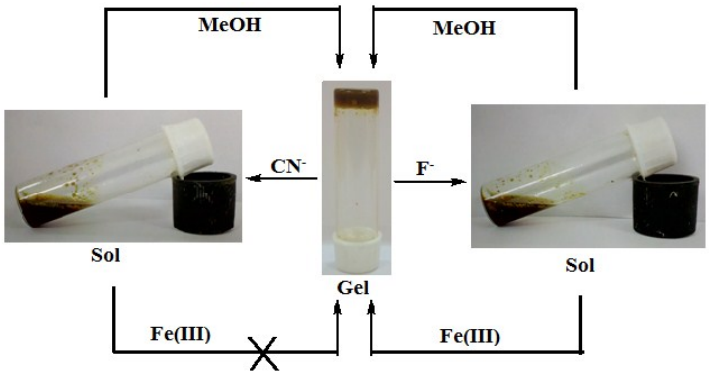

Fig. S10. Photograph showing the chemical reversibility of the anion induced sols of **2** in 1,2-dichlorobenzene and discrimination of F^- and CN^- ions.

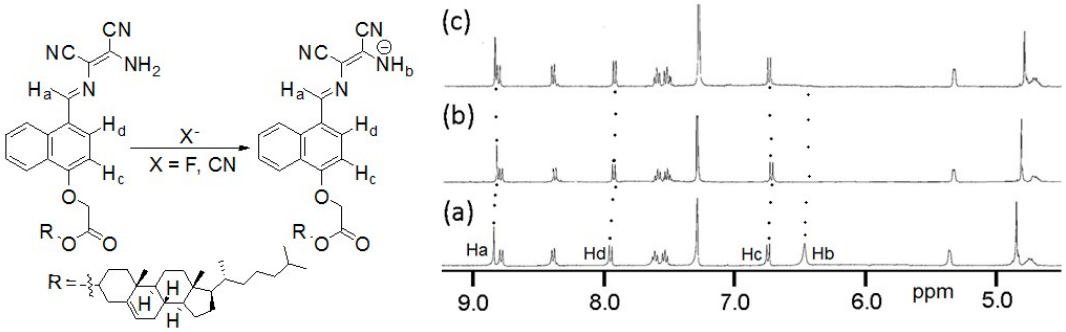

Fig. S11. Partial ^{1}H NMR spectra of **1** (a) in absence and in presence of equiv. amount of (b) F^- and (c) CN^- ions in $CDCl_3$ containing 5% d_6-DMSO.

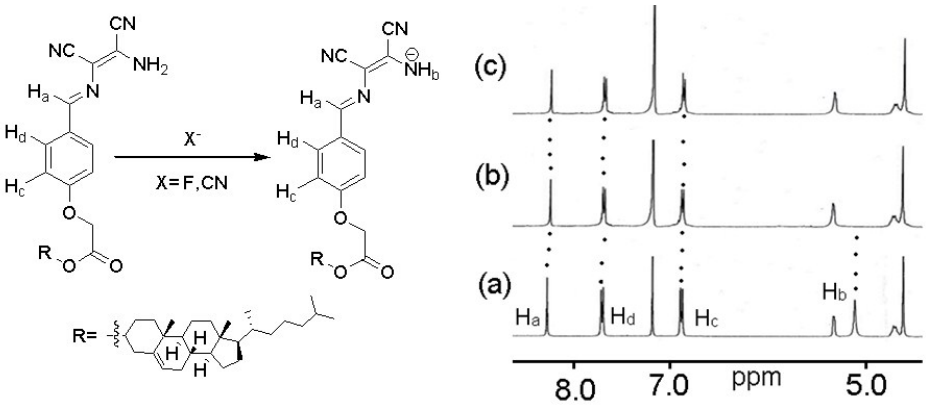

Fig. S12. Partial ^{1}H NMR spectra of **2** (c = 5.60 x 10^{-3} M) (a) in absence and in presence of equiv. amount of (b) F^- and (c) CN^- in $CDCl_3$.

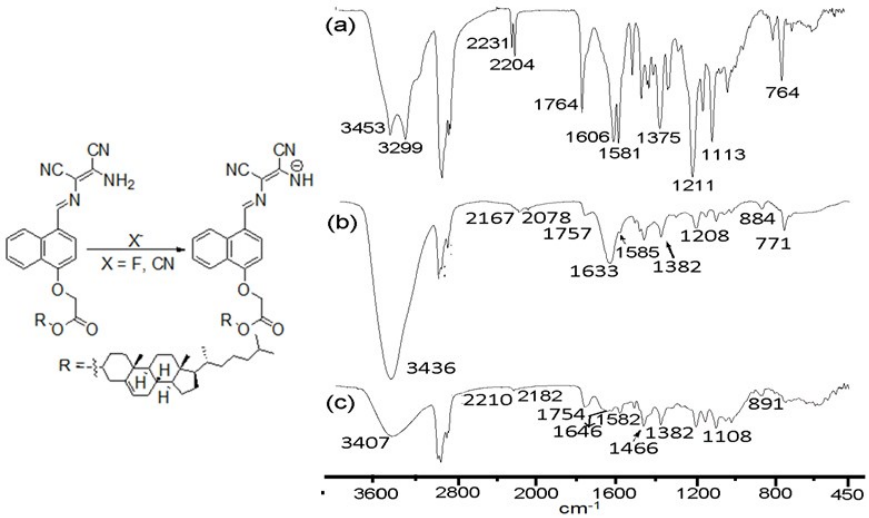

Fig. S13. Partial FTIR spectra of (a) **1**, (b) **1** with CN^- and (c) **1** with F^-.

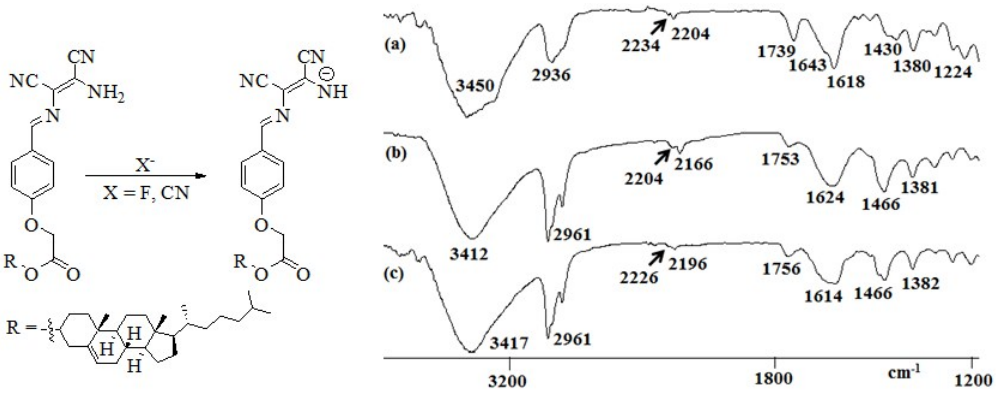

Fig. S14. Partial FTIR spectra of (a) **2**, (b) **2** with CN^- and (c) **2** with F^-.

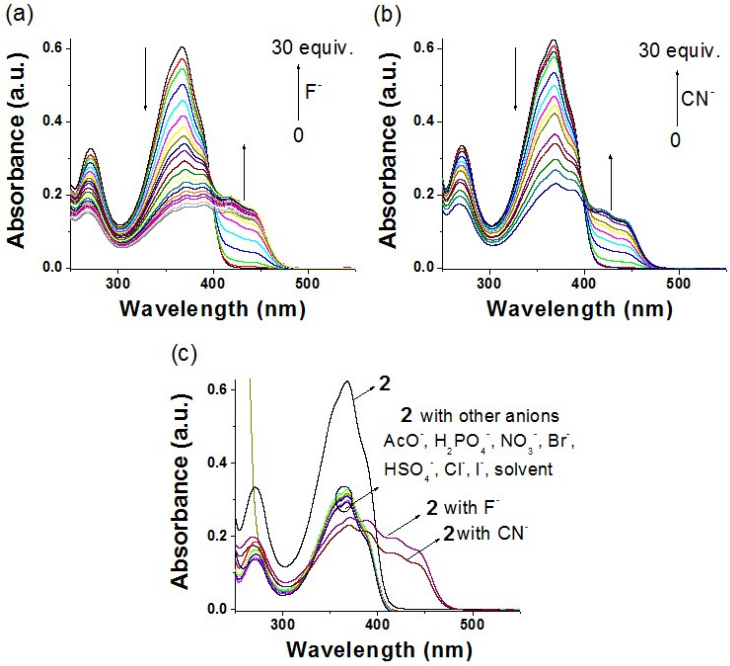

Fig. S15. Change in absorbance of **2** (c = 2.50 x 10^{-5} M) upon addition of 30 equiv. amounts of (a) F^-, (b) CN^- and (c) different anions (c = 1.0 x 10^{-3} M) in CH_3CN containing 1% DMF.

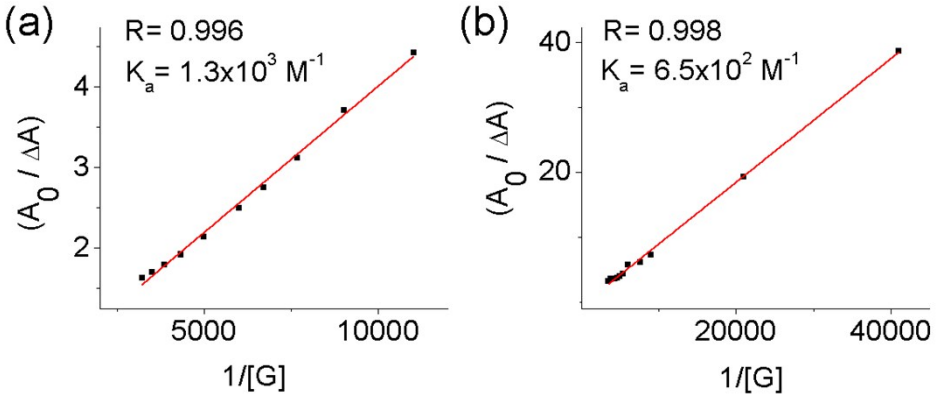

Fig. S16. Benesi–Hilderband plot for **1** (c = 2.5 x 10^{-5} M) with (a) CN^- and (b) F^- (c = 1.0 x 10^{-3} M) at 390 nm CH_3CN containing 0.5% DMF from UV-vis titration.

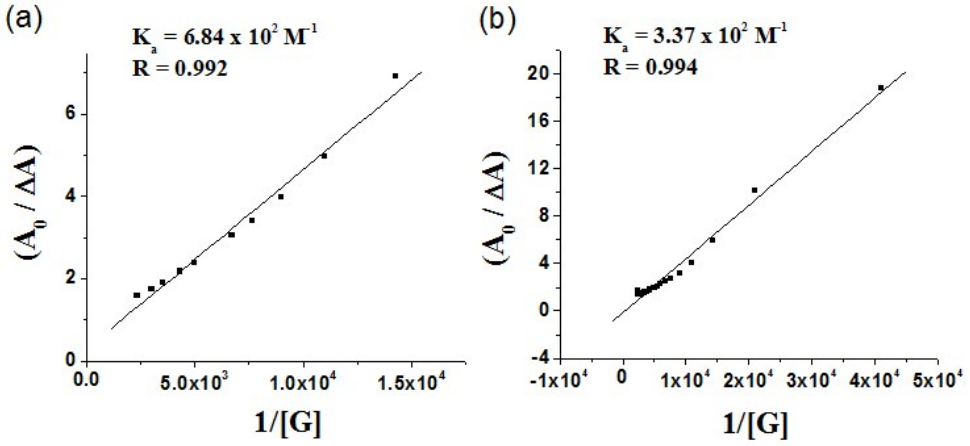

Fig. S17. Benesi–Hilderband plot for **2** (c = 2.5 x 10^{-5} M) with (a) CN^- and (b) F^- (c = 1.0 x 10^{-3} M) at 366 nm CH_3CN containing 1% DMF from UV-vis titration.

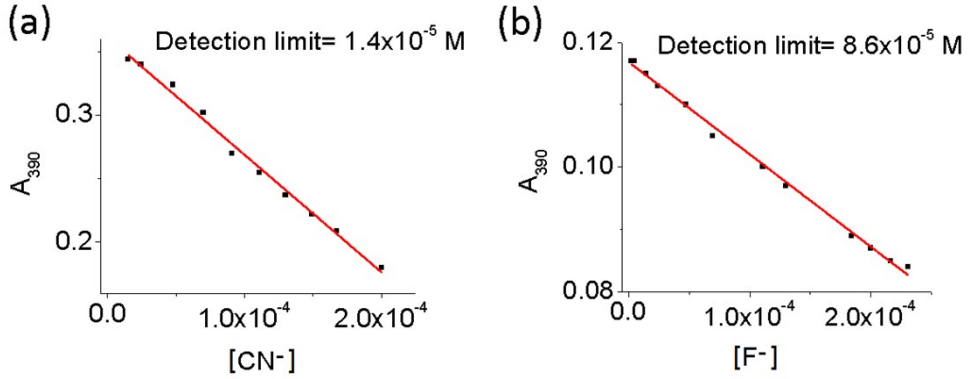

Fig. S18. Detection limit of (a) CN^- and (b) F^- for compound **1** at 390 nm in CH_3CN containing 0.5% DMF from UV-vis titration.

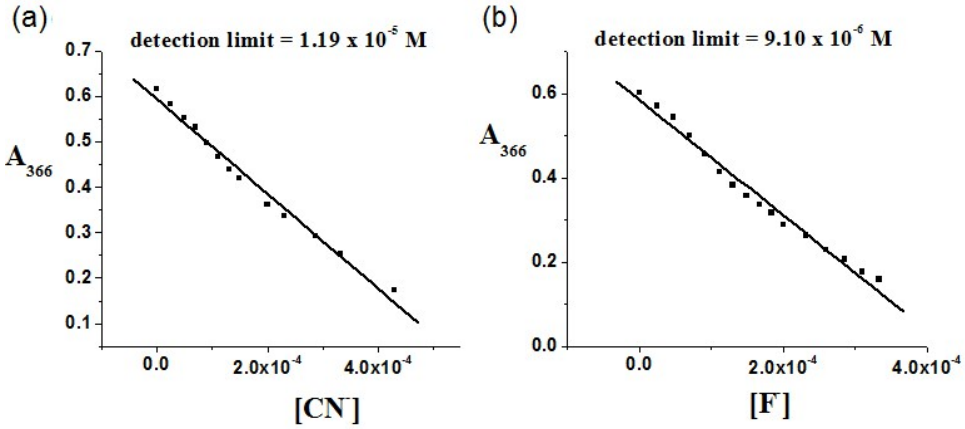

Fig. S19. Detection limit of (a) CN^- and (b) F^- for compound **2** at 366 nm in CH_3CN containing 1% DMF from UV-vis titration.

Table S2. Binding constants and detection limit values for the anion-ligand complexes.

Anion-ligand complex	Binding constant values (M^{-1})	
	From UV-vis titration	
1 – CN^-	K = 1.3 x 10^3	
1 – F^-	K = 6.5 x 10^2	
2 – CN^-	K = 6.84 x 10^2	
2 – F^-	K = 3.37 x 10^2	

Anion ligand complex	Detection limit values (M)	
	From UV-vis titration	
1 – CN^-	1.4 x 10^{-5}	
1 – F^-	8.6 x 10^{-5}	
2 – CN^-	1.19 x 10^{-5}	
2 – F^-	9.10 x 10^{-6}	

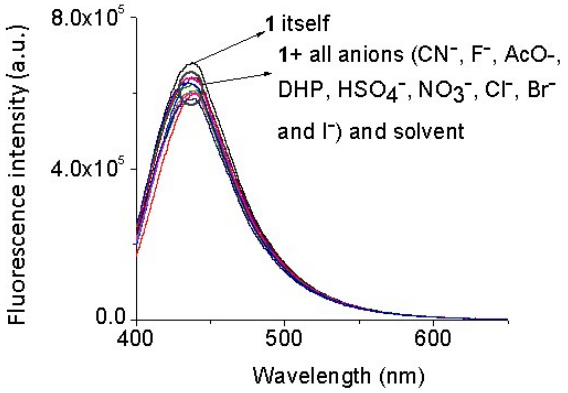

Fig. S20. Change in fluorescence intensity (λ_{ex} = 390 nm) of **1** (c = 2.50 x 10^{-5} M) upon addition of 16 equiv. amount different anions (c = 1.0 x 10^{-3} M) in CH_3CN containing 0.5% DMF.

Table S3: Reported structures for CN^- sensing in gel phase.

Entry	Gelator structure	Detection media	Sensing mechanism	solvent	Detection limit (M)	Interference from other anions	Ref.
1	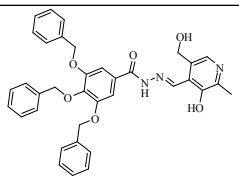	Gel-to-sol transition	H-bonding and Deprotonation	DMSO	-	F^- and AcO^-	2
2	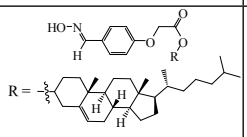	Gel-to-sol transition	H-bonding and Deprotonation	toluene	-	F^- and AcO^-	3
3	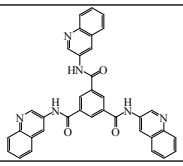	Gel-to-gel transition	H-bonding and Deprotonation	DMSO:H_2O (8:2, v/v)	-	F^-, AcO^- and $H_2PO_4^-$	4
4	Two component gel from citrazinic acid and melamine	Gel-to-sol transition	H-bonding and Deprotonation	Air dried gel	-	S^{2-}	5
5	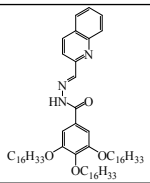	Gel-to-gel transition	Metal Displacement	DMF	1.0 x 10^{-5} 1.0 x 10^{-7}	-	6

6	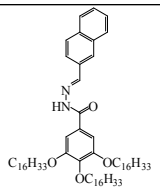	Gel-to-gel transition	Metal Displacement	EtOH	1.0×10^{-6}	-	7
7	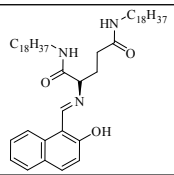	Gel-to-gel transition	Metal Displacement	DMSO	1.6×10^{-6}	-	8
8	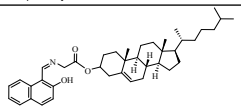	Gel-to-sol transition	Reaction-based	DMF:H_2O (2:1, v/v)	1.36×10^{-5}	-	9
9	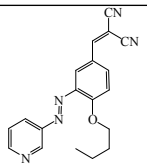	Gel-to-sol transition	Reaction-based	CH_3CN	9.36×10^{-6}	-	10
10	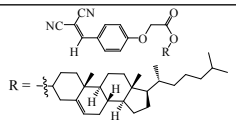	Gel-to-sol transition	Reaction-based	Toluene-CH_3OH (1:2, v/v)	4.17×10^{-6} (in CH_3CN)	-	3
11	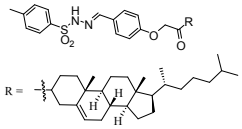	Gel-to-sol transition	H-bonding and Deprotonation	DMSO:H_2O (1:1, v/v)	7.96×10^{-5}	F^-	11
This work	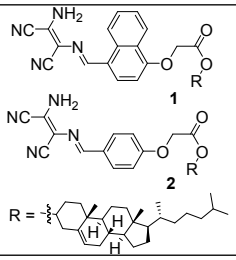	Gel-to-sol transition	H-bonding and Deprotonation	1a) toluene 1b) CH_3CN 2a) DCB 2b) CH_3CN	1a) - 1b) 1.4×10^{-5} 2a) - 2b) 1.19×10^{-5}	F^-	-

Table S4: Reported structures of diaminomalenonitrile-based anion-sensors.

Entry	Gelator structure	Detection media	solvent	Detection limit (M)	Responsiveness	Interference from other anions	Ref.
1	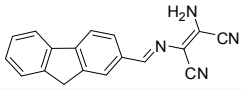	Solution	DMF:H_2O (4:1, v/v)	16nM	CN^-	F^-	12
2	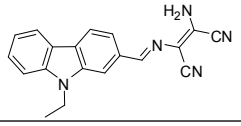	Solution	DMF	98nM	F^-	-	12
3	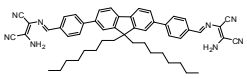	Solution	DMSO:HEPS buffer (1:4 v/v)	6.25 ×10−6	CN^-	-	13
4	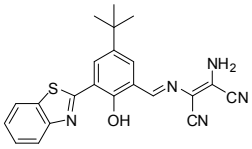	Solution	DMF:H_2O (1:1, v/v)	0.16 μM	CN^-	-	14
This work	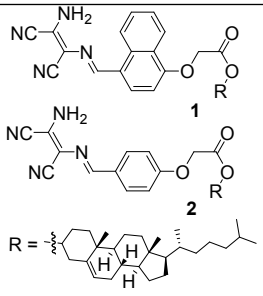	Gel-to-sol transition	1a) toluene 1b) CH_3CN 2a) DCB 2b) CH_3CN	1a) – 1b) 1.4 x 10^{-5} M 2a) – 2b) 1.19 x 10^{-5} M	CN^-	F^-	-

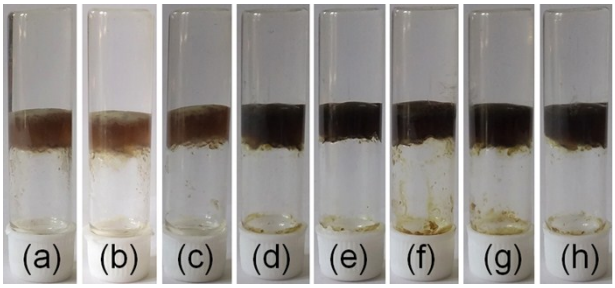

Fig. S21. Phase-selective gelation of **2** from biphasic mixture of water and (a) petroleum ether, (b) hexane, (c) cyclohexane, (d) petrol, (e) diesel, (f) kerosene, (g) Pump oil and (h) silicon oil

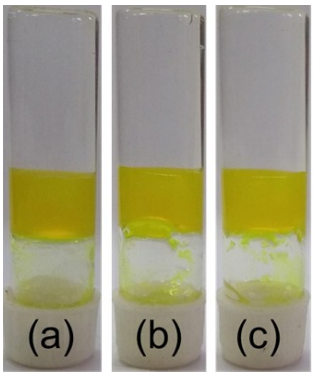

Fig. S22. Phase-selective gelation of **1** from toluene/water mixture in presence of (a) NaCl and from different water source (b) tap water and (c) river water.

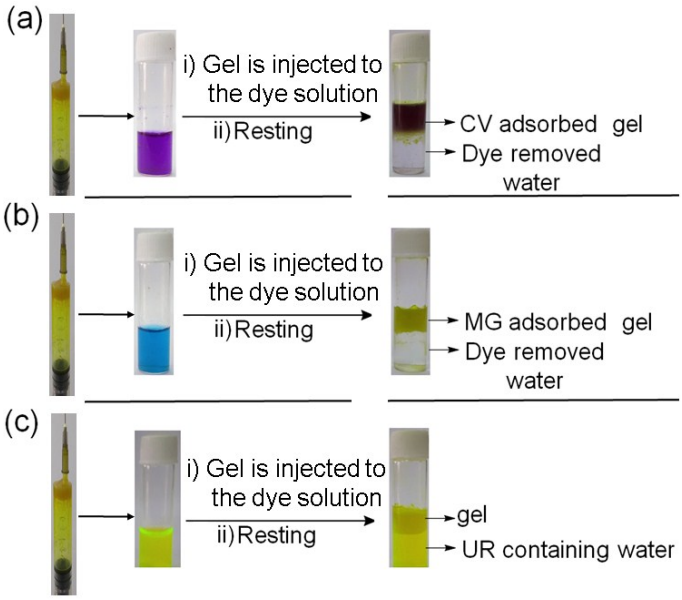

Fig. S23. Photograph showing the adsorption of (a) Crystal Violet (CV), (b) Malachite Green (MG), (c) Uranine (UR) when toluene gel of **1** (10 mg/mL) was injected to different dye solutions. In all cases, [dye] = 3.5 x 10^{-5} M.

.

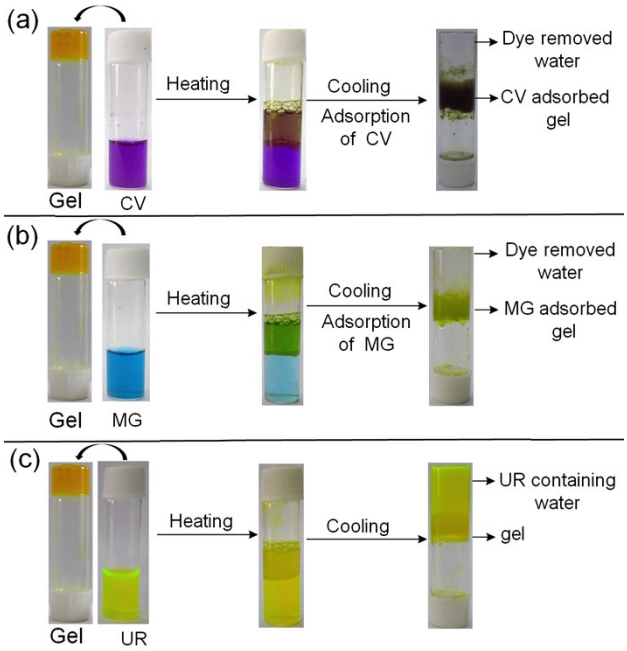

Fig. S24. Photograph showing the adsorption of (a) Crystal Violet (CV), (b) Malachite Green (MG), (c) Uranine (UR) by the toluene gel of **1** (10 mg/mL) *via* heating-cooling method. In all cases, [dye] = 3.5 x 10^{-5} M.

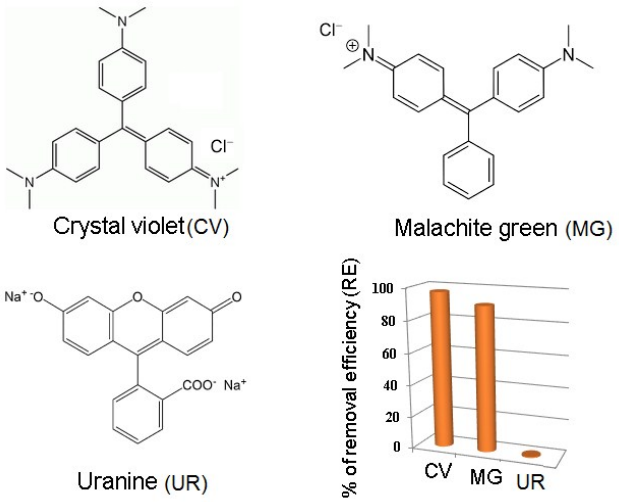

Fig. S25. Structures of dyes and the bar plot shows the respective adsorption data.

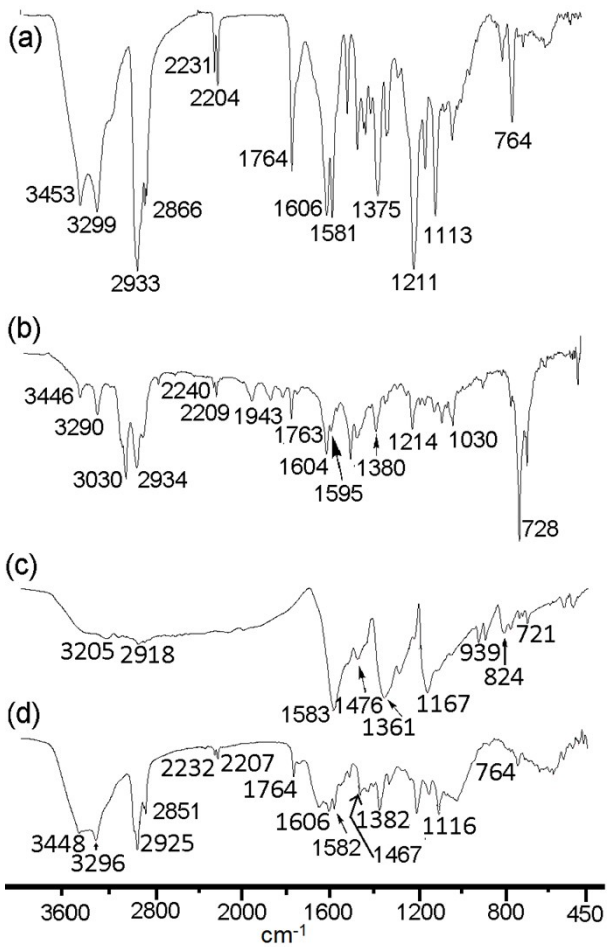

Fig. S26. Partial FTIR spectra of (a) **1** (amorphous) (b) toluene gel of **1**, (c) Crystal Violet and (d) Crystal Violet adsorbed gel.

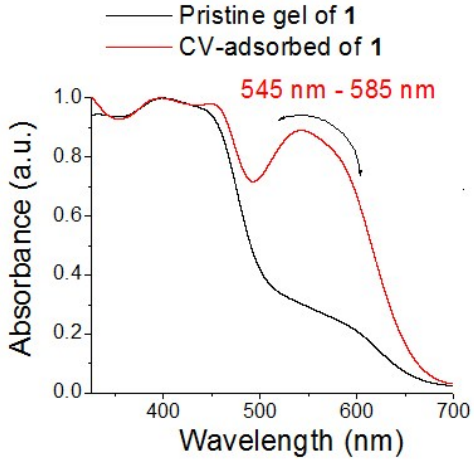

Fig. S27. Comparison of normalized UV-vis spectra of the toluene gel of **1** before and after adsorption of Crystal Violet (CV).

Table S5: Reported structures of supramolecular gelators applied in dye adsorption.

Entry	Gelator Structure	Dye removed	% of dye removed	Time Taken	Ref.
1.	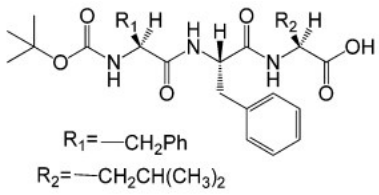	Rhodamine B (cationic dye) Reactive Blue 4 (neutral dye) Direct red 80 (anionic dye)	84 88 97	28h 30h 32h	15
2.	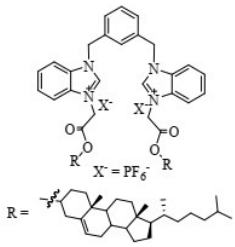	Uranine (anionic dye)	85	24h	16
3.	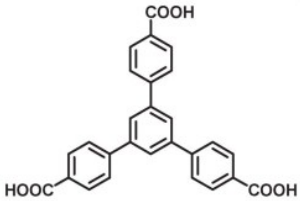	Rhodamine 6G (cationic dye) Crystal violet (cationic dye) Methylene Blue (cationic dye)	82.4 98.2 76.1	48h	17
4.	Ag(I)-melamine polymer hydrogel	Rose Bengal (neutral dye)	93	48h	18
5.	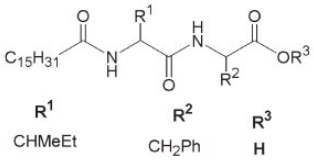	Crystal Violet (cationic dye)	97	24h	19
6.	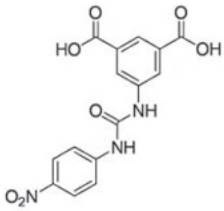	Methylene Blue (cationic dye) Methyl Violet 2B (cationic dye) 1-Pyrenemethylamine (neutral dye)	98 97 62	48h	20
7.	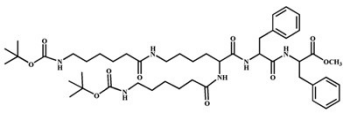	Crystal Violet (cationic dye)	>95	10h	21

8.	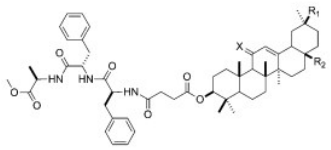	Rhodamine 6G (cationic dye) Acriflavine (cationic dye)	95 92	24h	22
9.	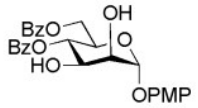	Methyl Violet 2b (cationic dye)	100	24h	23
10.	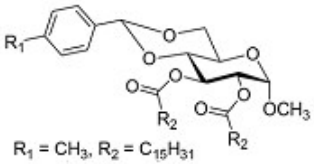	Crystal Violet Rhodamine B (both cationic dye)	>97	24h	24
11.	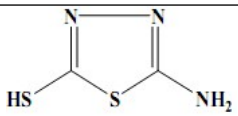 Ag^+-gel	Acid fuchsin (anionic dye)	95	4h	25
12.	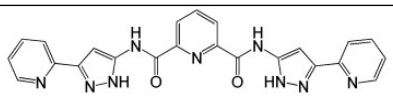 i) Ag^+-gel, ii) Cd^{2+}-gel, iii) Pb^{2+}-gel	Methyl orange (anionic dye)	i) 94	4h 24h 5h	26
13.	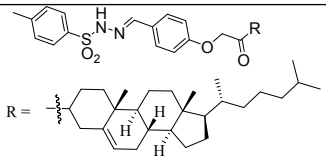	Erythrosine B Uranine (both anionic dye)	83 82	2h	11
This work	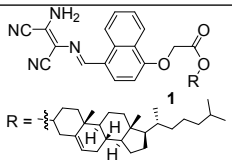	Crystal Violet Malachite Green (both anionic dye)	>97 >90	Within a minute	-

^{1}H NMR ($CDCl_3$, 400 MHz)

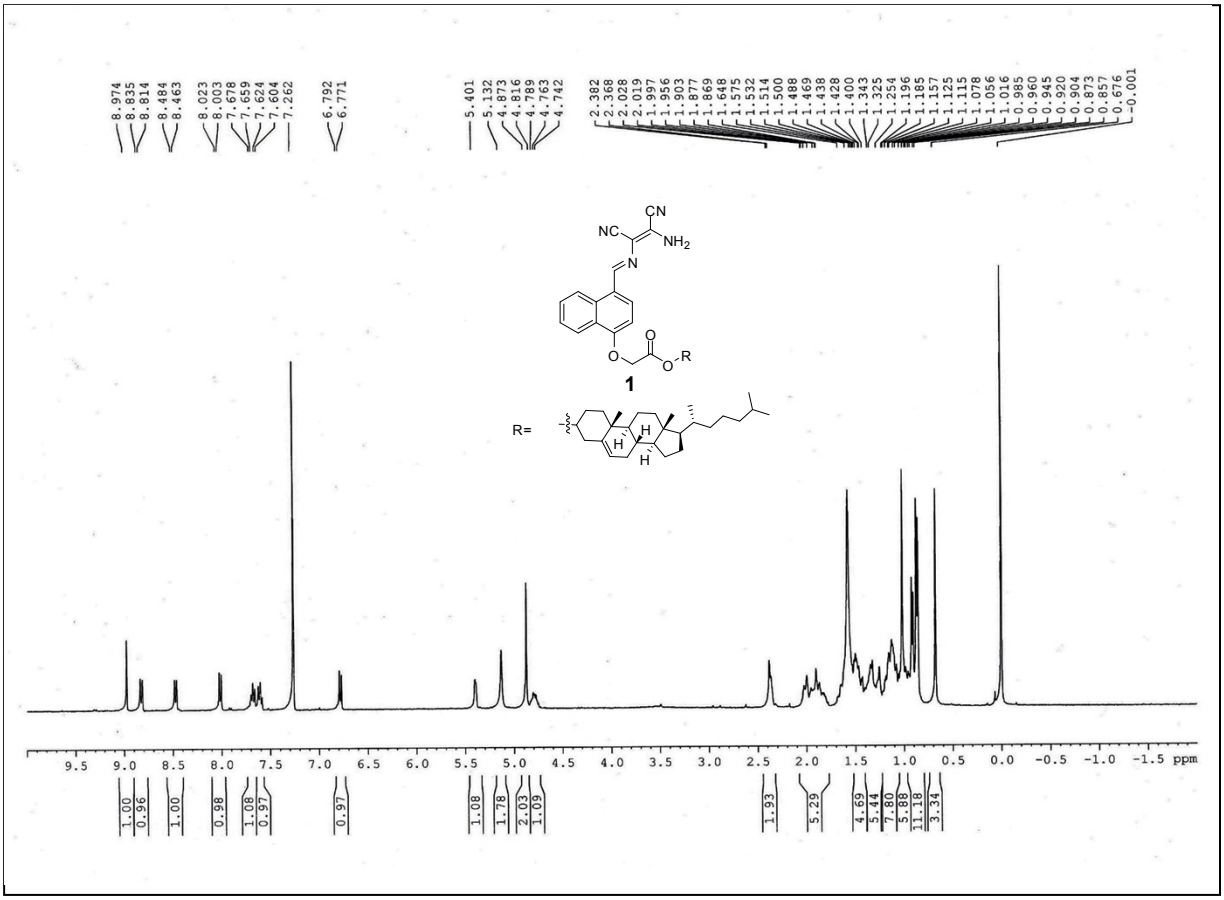

^{13}C NMR ($CDCl_3$ containing 40μL d_6-DMSO, 400 MHz)

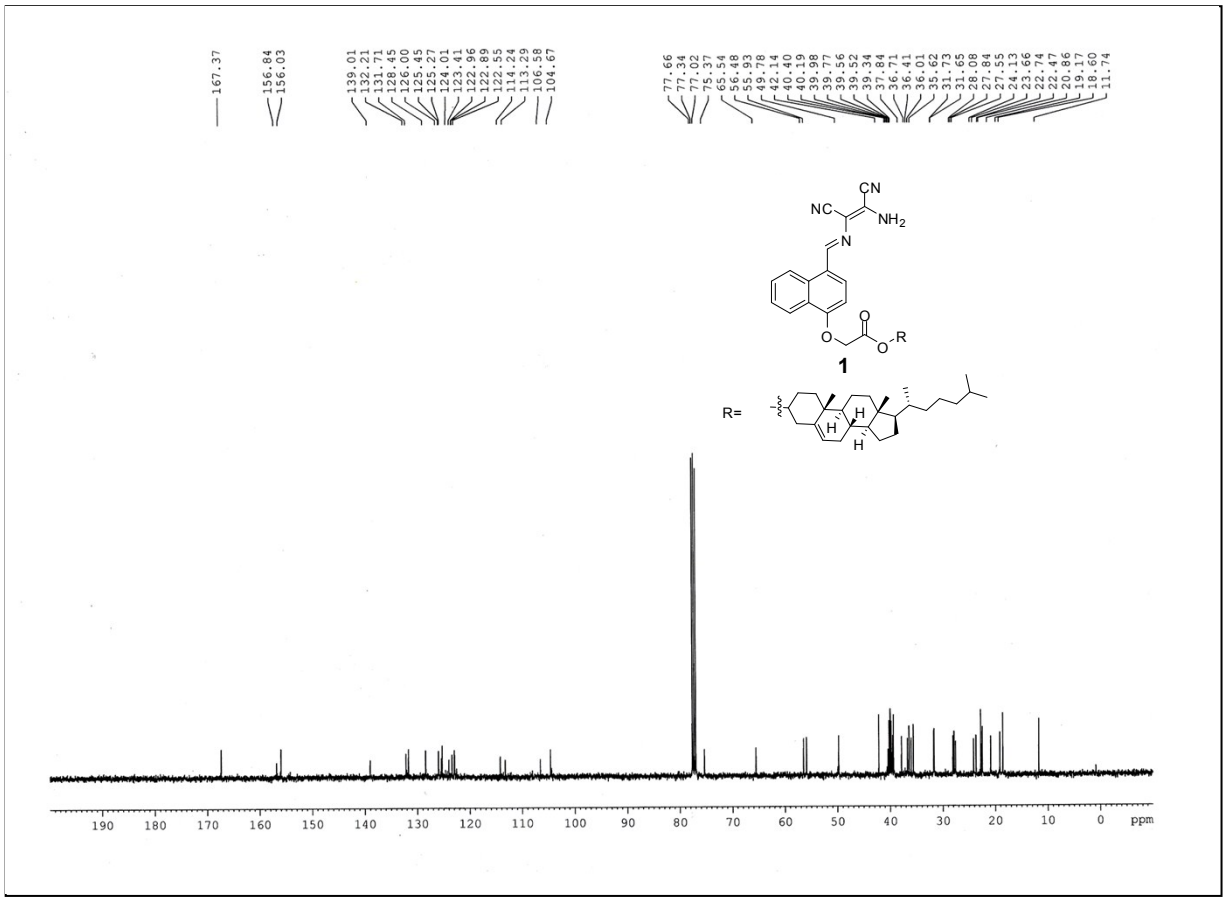

Mass spectrum of 1.

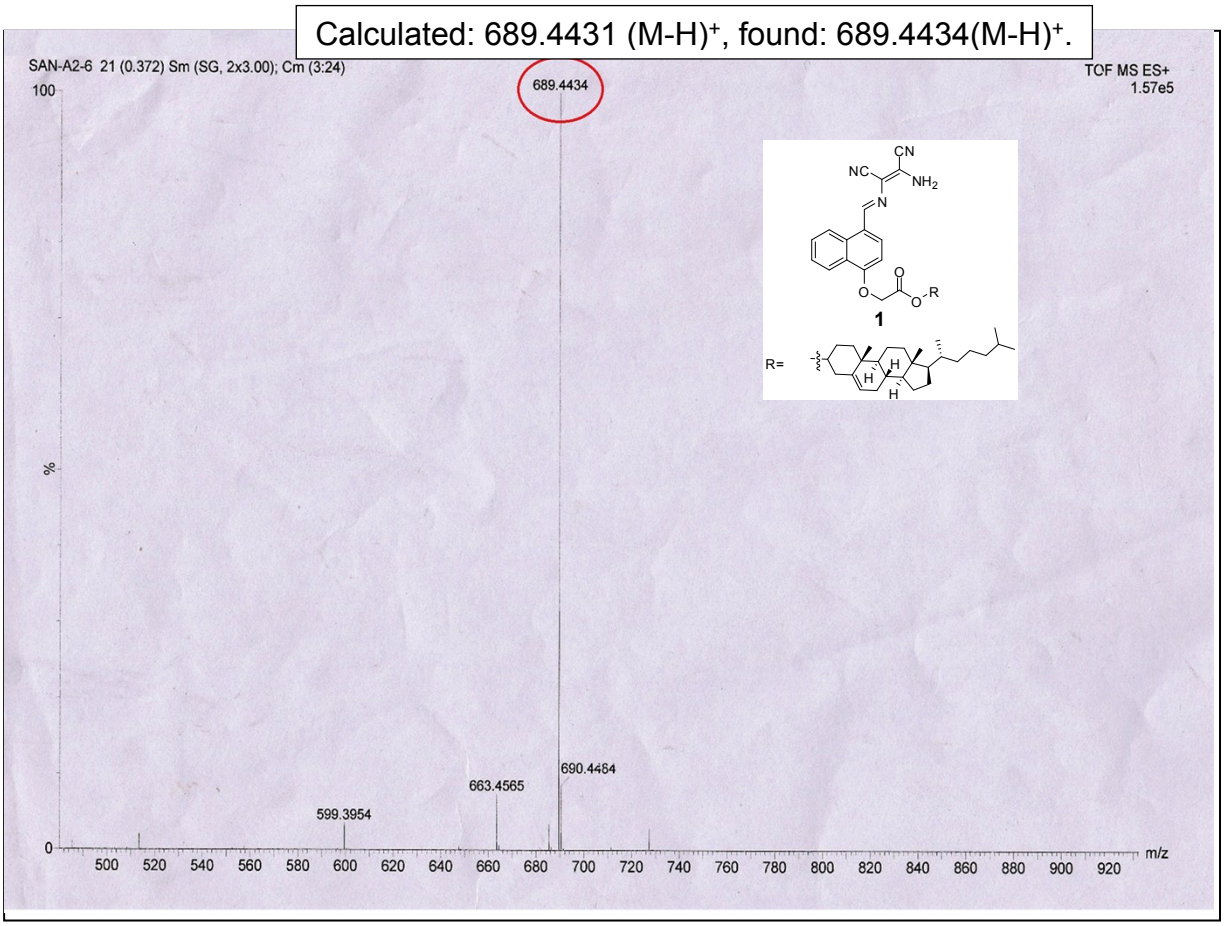

^{1}H NMR ($CDCl_3$, 400 MHz)

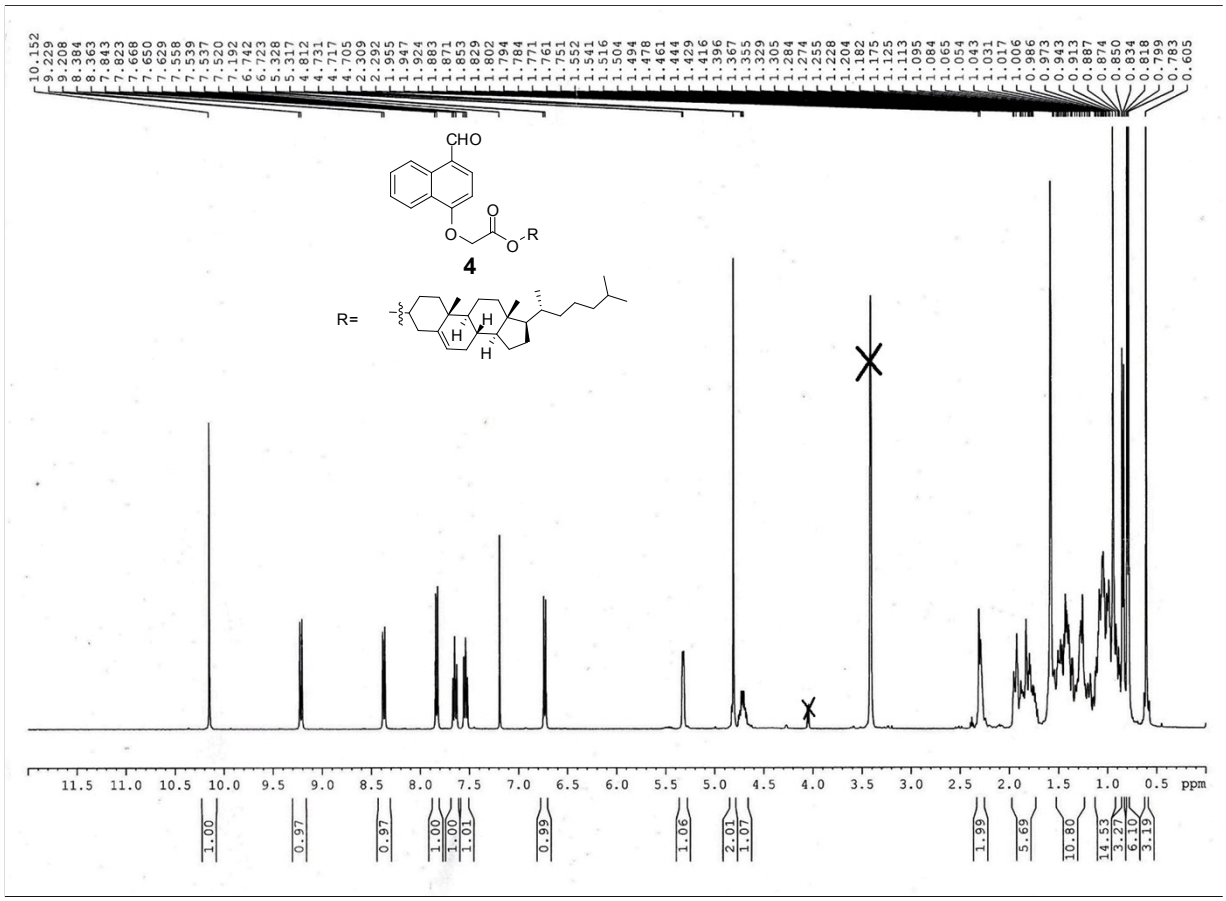

^{13}C NMR ($CDCl_3$, 400 MHz)

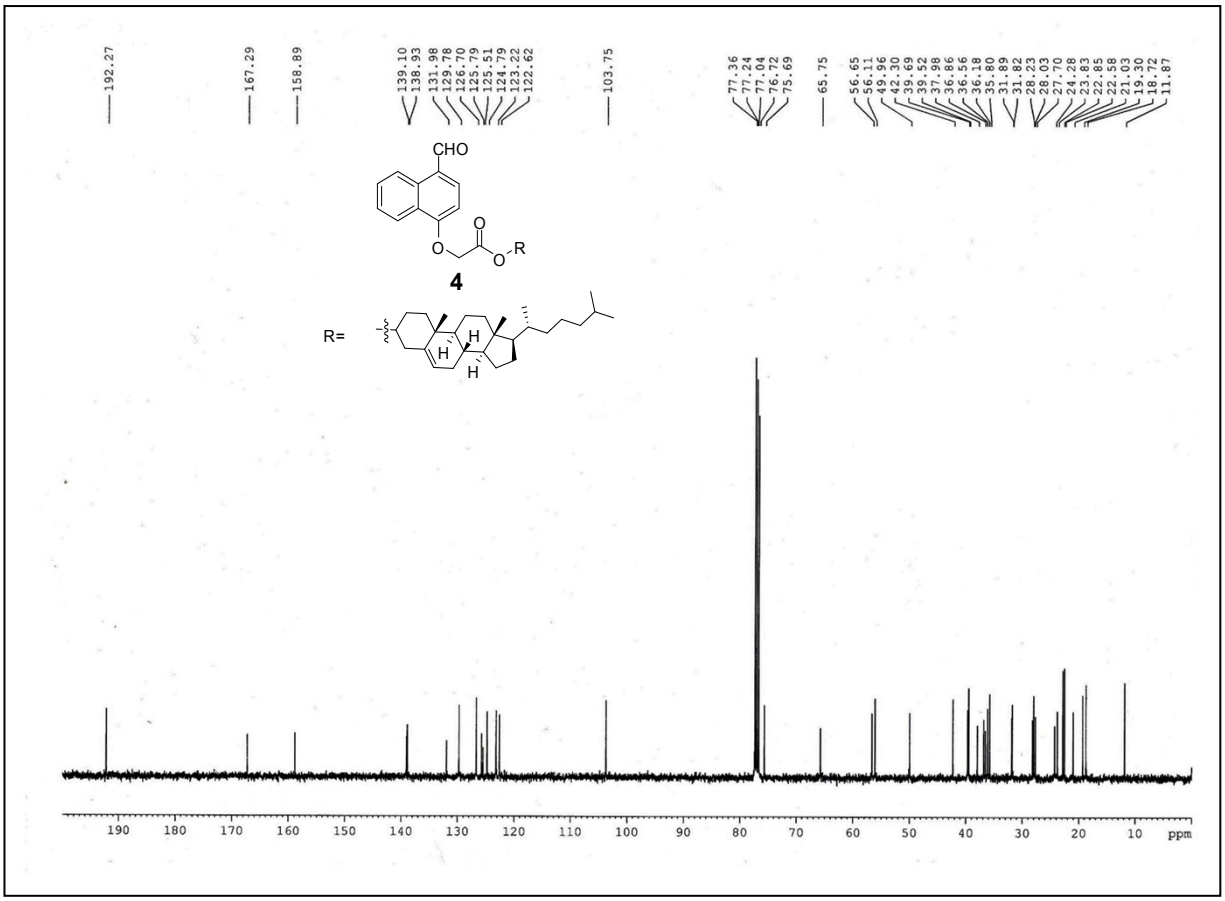

References

1. A. Panja and K. Ghosh, *New. J. Chem*., 2018, **42**, 13718-13725.
2. K. Ghosh and C. Pati, *Tetrahedron Lett*., 2016, **57**, 5469-5474.
3. A. Panja and K. Ghosh, *Supramol. Chem*., 2019, **31**, 239-250.
4. A. Ghosh, P. Das, R. Kaushik, K. K. Damodaran and D. A. Jose, *RSC Adv*., 2016, **6**, 83303-83311.
5. S. Sarkar, S. Dutta, C. Ray, B. Dutta, J. Chowdhury and T. Pal, *Cryst.Eng.Comm*., 2015, **17**, 8119-8129.
6. Q. Lin, B. Sun, Q. P. Yang, Y. P. Fu, X. Zhu, T. B. Wei and Y. M. Zhang, *Chem. Eur. J*., 2014, **20**, 11457-11462.
7. Q. Lin, T. T. Lu, X. Zhu, B. Sun, Q. P. Yang, T. B. Wei and Y. M. Zhang, *Chem. Commun*., 2015, **51**, 1635-1638.
8. J. Sun, Y. Liu, L. Jin, T. Chen and B.Yin, *Chem. Commun*., 2016, **52**, 768-771.
9. K. Ghosh and S. Panja, *Supramol. Chem*., 2017, **29**, 350-359.
10. A. Panja and K. Ghosh, *Chemistry Select*, 2018, **3**, 1809-1814.
11. A. Panja, S. Ghosh and K. Ghosh, *New. J. Chem*., 2019, **43**, 10270-10277.
12. S. Sarveswari, A. J. Beneto and A. Siva, *Sens. Actuators, B*., 2017, **245**, 428–434.
13. M. J. Kim, R. Manivannan, I. J. Kim, and Y. A. Son, *Sens. Actuators, B*., 2017, **253**, 942–948.
14. K. Keshav, P. Torawane, M. K. Kumawat, K. Tayade, S. K. Sahoo, R. Srivastava and A. Kuwar, *Biosens. Bioelectron*., 2017, **92**, 95–100.
15. B. Adhikari, G. Palui and A. *Soft Matter*, 2009, **5**, 3452-3460.
16. S. Panja, S. Bhattacharya and K. Ghosh, *Langmuir*, 2017, **33,** 8277-8288.
17. P. K. Sukul and S. Malik, *RSC Adv*., 2013, **3**, 1902-1915.
18. P. Bairi, B. Roy and A. K. Nandi, *J. Mater. Chem*., 2011, **21**, 11747-11749.
19. T. Kar, S. Debnath, D. Das, A. Shome and P. K. Das, *Langmuir*, 2009, **25**, 8639-8648.
20. F. R. Llansola, B. Escuder, J. F. Miravet, D. H. Merino, I. W. Hamley, C. J. Cardin and W. Hayes, *Chem. Commun*., 2010, **46**, 7960-7962.
21. T. Kar, S. Mukherjee and P. K. Das, *New J. Chem*., 2014, **38**, 1158-1167.
22. J. Lu, Y.Gao, J.Wua and Y. Ju, *RSC Adv*., 2013, **3**, 23548- 23552.
23. K. B. Pal and B. Mukhopadhyay, *ChemistrySelect*, 2017, **2**, 967-974.
24. X. Zhang, J. Song, W. Ji, N. Xu, N. Gao, X. Zhang and H. Yu, *J. Mater. Chem. A*., 2015, **3**, 18953-18962.
25. Y. Cheng, Q. Feng, M. Yin, X. Ren, J. Wang and Y. H. Zhou, *New J. Chem*., 2016, **40**, 9125-9131.
26. (a) S. Sengupta, A. Goswami and R. Mondal, *New. J. Chem*., 2014, **38**, 2470-2479; (b) S. Sengupta and R. Mondal, *J. Mater. Chem. A*., 2014, **2**, 16373-16377.